INFLUENCE OF TWO-PRONG INELASTIC EVENTS ON (π^+ ^{3}He) REACTION AT 120 MeV

UBPub. EPPG/Phys. 35
November 1996

T. Angelescu, I. Lazanu, A. Mihul, L. Teodorescu
Bucharest University - Bucharest, Romania

R. Ionica
"Politehnica" University - Bucharest, Romania

R. Garfagnini
Instituto di Fisica Generale dell'Universita - Torino, Italy

T. Preda, Yu. Shcherbakov
Joint Institute for Nuclear Research - Dubna, Russia

SUMMARY

A detailed study of the two-prong inelastic events from the (π^+ ^{3}He) scattering at 120 MeV kinetic energy has been realised. The results are used together with our previously analysed three-prong events to interpret the inelastic channels of this interaction.

The results show that the two-prong inelastic events are mainly distributed in the scattering channels (22.5% πpd and 75.5% 4-particle final state). The inelastic cross-sections have been calculated. The dominant mechanism for describing the πpd final state reaction is the knock-out one.

PACS. 13.75. - Hadron-induced low- and intermediate-energy reactions and scattering, energy ≤ 10 GeV.

INFLUENCE OF TWO-PRONG INELASTIC EVENTS ON (π^+ ^{3}He) REACTION AT 120 MeV

T. Angelescu, I. Lazanu, A. Mihul, L. Teodorescu
Bucharest University - Bucharest, Romania

R. Ionica
"Politehnica" University - Bucharest, Romania

R. Garfagnini
Instituto di Fisica Generale dell'Universita - Torino, Italy

T. Preda, Yu. Shcherbakov
Joint Institute for Nuclear Research - Dubna, Russia

SUMMARY

A detailed study of the two-prong inelastic events from the (π^+ ^{3}He) scattering at 120 MeV kinetic energy has been realised. The results are used together with our previously analysed three-prong events to interpret the inelastic channels of this interaction.

The results show that the two-prong inelastic events are mainly distributed in the scattering channels (22.5% πpd and 75.5% 4-particle final state). The inelastic cross-sections have been calculated. The dominant mechanism for describing the πpd final state reaction is the knock-out one.

PACS. 13.75. - Hadron-induced low- and intermediate-energy reactions and scattering, energy ≤ 10 GeV.

1. Introduction

The interaction of pions with light nuclei in the Δ_{33} resonance energy region has been investigated in many experiments using different kinds of detectors. However, those experiments using detectors with track visualisation seem to have some advantages for this study. The analysis of the inelastic events with three or four particles in the final state can not be performed in one-arm spectrometer experiments while the two-arm spectrometer is too expensive. The cheapest detector is a triggered streamer chamber which can give a complete information about charged particles and the limit in the momentum detection is low (30 MeV/c for protons and 50MeV/c for deuterons).

Such an experiment has been realised at JINR-Dubna using a self-shunted streamer chamber filled with ^{3}He at 4 atm pressure and a pion beam with the kinetic energy between 68 and 208 MeV. The experimental apparatus has been described in detail in ref. [1]. The pictures obtained have been analysed for elastic and inelastic channels and some results have been published in ref.[2,3,4]. In the previous analysis of the inelastic channels a part of the events have not been included due to the lack of information on one particle with a too low momentum to be registered in the chamber. These two-prong unprocessed inelasic events have been taken into account in cross section computation as a general correction. The processing of these events can give a more complete scenario about the reaction mechanisms and the inelastic cross section contribution in different channels.

In the present paper we give a method for processing two-prong inelastic events. This analysis will complete a phase space region which was not covered in the previous analysis and permits us a discussion about the reaction mechanisms and their contribution. The distributions have been interpreted using two reaction mechanisms: the knock-out of a proton or a virtual deuteron inside the nucleus by the incident pion and the compound mechanism.

The experimental material for (π^+ ^{3}He) scattering at 120 MeV kinetic energy has been used.

2. Experimental Method

The experimental sample contains events from two different exposures of the streamer chamber on a positive-pion beam of 120 MeV kinetic energy. The present analysis has been made only for two-prong events. Three-prong events have already been analysed and we will use the published data [4] in our further discussion.

A number of 296 two-prong events (213 inelastic and 83 elastic events) has been recorded. They have been processed by programs for geometrical reconstruction,

kinematics and fitting the possible hypotheses on the reaction channels. The algorithms of these programs are extensions of those used for the three-prong events [5,6] including changes for the new event topologies (only two particles in the final state for the elastic events and a proton momentum lower than 30 MeV/c or a deuteron momentum lower than 50 MeV/c for the two-prong inelastic events).

In order to separate the different channels and also the different possibilities of the assignment of the particles to the tracks for the πpd final state, the following elements have been used:

-the energy dispersion (ΔE) for the corresponding mass assignment

-the momentum dispersion (Δp_z) of the third momentum projection

-the coplanarity of the elastic events expressed through $\Delta\theta = \theta_{13} + \theta_{12} - \theta_{23}$, where θ_{ij} is the angle between particles i and j.

The corresponding criteria have been used in the following way:

-events for which $|\Delta E| \leq 10$ MeV and $|\Delta\theta| \leq 4.5°$ have been considered as elastic events,

-events for which $|\Delta E| \leq 50$ MeV and $|\Delta p_d| \leq 60$ MeV/c have been considered three particle events (πpd or ppp final state).

The events for which no hypothesis had fulfilled these conditions have been considered four particle events (π^+ppn or π^0ppp final state).

Finally, for the fitted hypotheses, the computed particle energy loss has been compared with the ionisation and the computed range with the presumed length of the track.

We have selected up to three hypotheses for each event and a corresponding weight ($1/N_{hyp}$) has been introduced for each hypothesis. The geometry and the triggering efficiency of the system have been considered through a geometric weight for each event [5].

Once the assignment of the particles to the tracks done, the direction and the momentum of the unseen charged particle have been determined from the momentum conservation.

3. Results and Discussion

3.1 Cross Sections

The elastic events have been analysed in detail in ref. [2] and we will not discuss them here any more.

The inelastic cross sections have been computed using the formula

$$\sigma = N_{corr}\ w\ \eta$$

where

N_{corr} is the number of the measured events, corrected for the different losses,

w is the average weight of one event for the corresponding reaction; it takes into account the geometrical and triggering corrections [5,6],

η is the millibarn equivalent of the exposure.

The number of the measured events has been corrected for the following losses:

- events lost due to the bad quality of the photographs (α_1),
- events lost at the edge of the effective volume of the chamber (α_2),
- scanning efficiency loss (α_3).

Table I

Exp.	*η (mb/even)*	α_1	α_2	α_3	$w_{\pi pd}$	w_{ppp}
I	0.052	0.19±0.02	0.16±0.02	0.03±0.01	5.12	5.85
II	0.138	0.19±0.03	0.23±0.04	0.03±0.01	5.04	4.35

The correction factors for these losses are presented in the Table I as well as the values of η and w. The values are presented separately for the two exposures of the chamber (noted I and II).

Table II

Reaction	*Nr. events*		*Cross sections*
	3prong	*2prong*	*(mb)*
πpd	54	48	31.4±3.3
ppp	15	4	14.4±2.1
unidentified	33	0	—
4-part.	193	161	103.5±6.5
total inel.	295	213	149.3±7.6

The number of the measured inelastic events and the inelastic cross sections, calculated adding the present analysed two-prong inelastic events and the previously obtained [4] three-prong events, are shown in the Table II. The unidentified events, presented in the table, are those with all three prongs in a plane or those with a secondary track along the stereobasis. It has been demonstrated in ref. [5] that these events belong mainly to the ppp final state. Our cross section value for the ppp channel includes these unidentified events. So, it has to be considered as a maximum value.

Two-prong inelastic events are distributed mainly in the scattering channels, (22.5+/-3.6)% as πpd final state and (75.5+/-7.9)% as four-particle final state, and only few in the absorption channel, (2.0+/-0.9)%. We will discuss further only the

πpd channel because of the small number of the two-prong absorption events and because we have complete information only for the three-particle final state.

3.2 Momentum and Angular Distributions

In all following figures we show the distributions of the summed two- and three-prong inelastic events and the corresponding statistical uncertainties. The hatched area represents the contribution of the three-prong events. In the same figures we also show the result of a Monte Carlo simulation of the knock-out process.

In our Monte Carlo simulation we have considered that the incident pion would have a quasi-elastic interaction only with a proton or a virtual deuteron inside the ^{3}He nucleus (the participant particle) and the remainder of the nucleus (the spectator particle) would not participate at the interaction. The quasi-elastic interaction of the pion with the participant particle has been described using the results of the phase shift analysis at the corresponding energy [7]. As the momentum distribution of the spectator particle we have used a Hulthen potential [8]. We have also taken into account the cuts introduced by the triggering system.

The distributions for the proton and the deuteron have always been summed because of the existing ambiguity in the separation between these particles.

a. Momentum distributions

In figure 1 we present the momentum distributions of the secondary particles in the centre-of-mass and laboratory systems.

The analysis of these spectra can be done using the two possible mechanisms: the knock-out of a proton or a virtual deuteron inside the ^{3}He nucleus by the incident pion (KO) and the compound mechanism, i.e. the excitation of the nucleus with the subsequent decay. The last mechanism gives a distribution well represented by the three particle phase space (PS).

The high momentum peak in the pion momentum distributions is owing to the KO mechanism as can be seen from the Monte Carlo calculation. The experimental values represented in figure 1a have been fitted with a PS distribution in the region $p_\pi^* < 140$ MeV/c. This fit has shown that less than 4% of the events occur owing to a PS mechanism. Comparing this value with those obtained for the pion scattering at 145 MeV (16%) and 180 MeV (15%) where only the three-prong events have been used, we can conclude that the two-prong events are mainly generated by a KO mechanism.

b. Angular distributions

Figure 2 shows the angular distributions of the secondary particles in the centre-of-mass and laboratory systems.

The lack of events in the regions $\theta_\pi < 30°$, $\theta_\pi > 150°$ and $\theta_{p,d} < 10°$ is due to the cut operated by the triggering system. The high backward peak in the centre-of-mass angular distribution of the heavy particles (fig. 2c) is given by the two-prong inelastic events, in

agreement with the Monte Carlo calculation showing that these events are mainly produced by a KO process.

c. Angular correlations

In the figures 3a and 3b we show the distributions of the angle between the proton and the deuteron in the centre-of-mass and laboratory systems. Better agreement with the Monte Carlo calculation is obtained by completing the sample with two-prong inelastic events.

The figures 3c and 3d show the distributions of the opening angle between the scattered pion and one of the heavy particles in the same centre-of-mass and laboratory systems. The two-prong events have a greater contribution at large angles in the centre-of-mass system. The backward accumulation of events is explained by the KO process.

Figure 4 shows the distributions of the azimuthal angle between the proton and the deuteron as well as of the azimuthal angle between the scattered pion and one of the heavy particles. These distributions are independent of the reference frame but they are not independent of the identification of the heavy particle (as it was for the three-prong events [3]) because the direction of the low momentum particle has been determined after the assignation of the particles to the tracks.

The concentration of events in the region $\varphi_{\pi p,\pi d} > 150°$ is an indication of the presence of the knock-out process, in agreement with the Monte Carlo simulation.

4. Conclusions

From the processing of the two-prong inelastic events we can conclude that:

a. The two-prong inelastic events are mainly distributed in the scattering channels (22.5% πpd and 75.5% 4-particle) and a very small fraction of them corresponds to the absorption channel (2%).

b. The pion scattering on ^{3}He at 120 MeV kinetic energy is described by two mechanisms: the knock-out of a proton or a virtual deuteron inside the nucleus by the incident pion (96%) and the compound mechanism (4%).

c. The two-prong inelastic events are mainly produced by the knock-out process. The Monte Carlo simulation for this process is in a good agreement with the experimental distributions completed with the two-prong inelastic events.

***

We are grateful to Dr. I. V. Falomkin, Dr. V. I. Lyashenko for their contribution to the early stage of the π^3He studies and the team that had built and run the experiment at JINR-Dubna.

REFERENCES

[1]. I. V. Falomkin, M. M. Kulyukin, V. I. Lyashenko, F. G. Nichitiu, G. B. Pontecorvo, Yu. A. Shcherbakov, G. Piragino., Lett. Nuovo Cimento, **3**, 461 (1972);

[2]. Yu. A. Shcherbakov, T. Angelescu, I. V. Falomkin, M. M. Kulyukin, V. I. Lyashenko, R. Mach, A. Mihul, N. M. Kao, F. Nichitiu, G. B. Pontecorvo, V. K. Sarycheva, M. G. Sapozhnikov, M. Semerdjieva, T. M. Troshev, N. I. Trosheva, F. Balestra, L. Busso, R. Garfagnini, G. Piragino, Nuovo Cimento A, **31**,262 (1976);

[3]. T. Angelescu, I. Lazanu, A. Mihul, L. Pascu, I. V. Falomkin, G. B. Pontecorvo, Yu. A. Shcherbakov, R. Ionica, R. Garfagnini, G. Piragino, Il Nuovo Cimento A, **89**, 162 (1985); **100**, 381 (1988);

[4]. A. Mihul, T. Angelescu, R. Ionica, Yu. Shcherbakov, I. Lazanu, T. Preda, R. Garfagnini, Il Nuovo Cimento A **103**, 93 (1990); **105**, 1637 (1992);

[5]. T. Angelescu, A. Mihul, L. Pascu, I. Lazanu, R. Ionica, R. Garfagnini, G. Piragino, V. I. Lyashenko, I. V. Falomkin, Yu. A. Shcherbakov, Rev. Roum. Phys. **31**, 125 (1986);

[6]. F. Balestra, S. Bossolasco, M. P. Bussa, L. Busso, L. Ferrero, G. Gervino, D. Panziery, G. Piragino, F. Tosselo, I. V. Falomkin, V. I. Lyashenko, G. B. Pontecorvo, Yu. A. Sherbakov, D Cauz, R. Garfagnini, L. Santi, A. Maggiora, Lett. Nuovo Cimento, **41**, 391 (1984);

[7]. W.O. Lock, High energy nuclear physics, N.Y., 1960;

[8]. W. J. Thompson, W.R. Hering, Phys. Rev. Lett., **24**, 272 (1970);
L. Hulthen, M. Sugarava, Handb. Phys., **39**, 1 (1957).

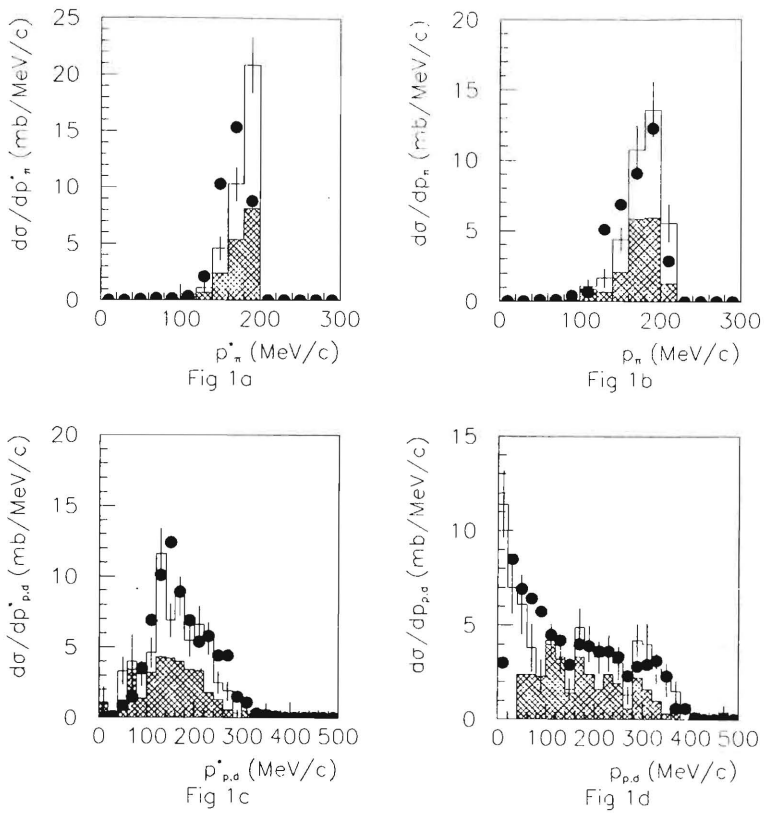

Fig 1. Momentum distributions of the secondary particles: pion momentum distributions in C.M.S. (a) and L.S. (b), heavy particle momentum distributions in C.M.S. (c) and L.S. (d). The points are the results of the Monte Carlo calculation.

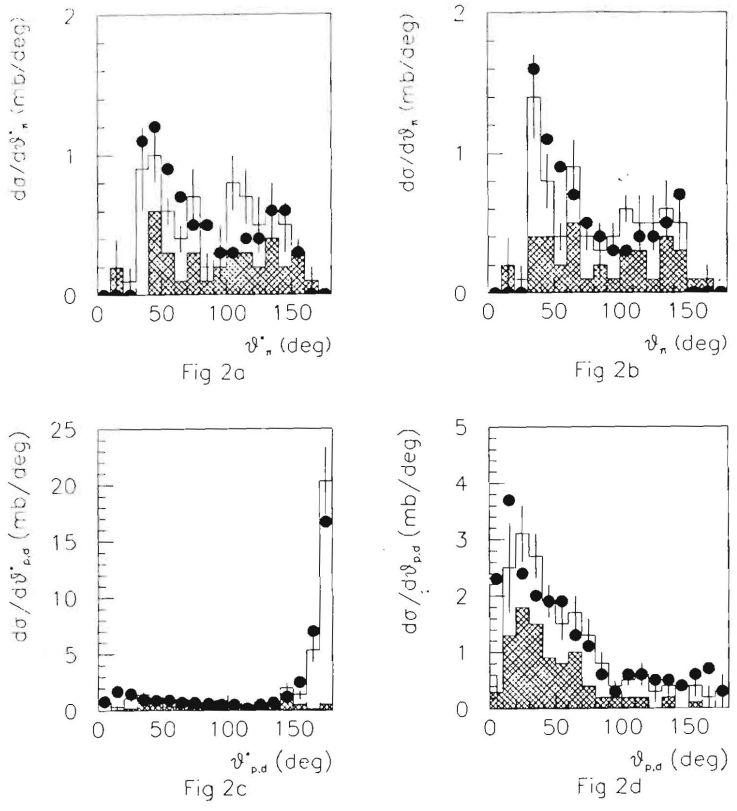

Fig 2. Angular distributions of the secondary particles: pion distributions in C.M.S. (a) and L.S. (b), heavy particles distributions in C.M.S. (c) and L.S. (b). The points as in fig.1.

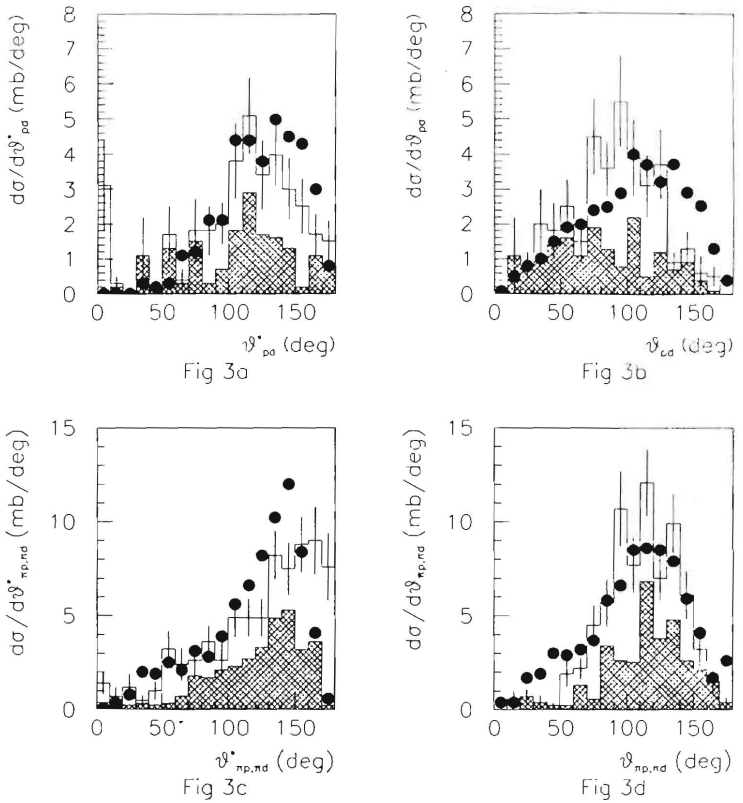

Fig 3. Opening angle θ_{ij} distributions of the secondary particles in C.M.S. (a,c) and L.S. (b,d). The points as in fig 1.

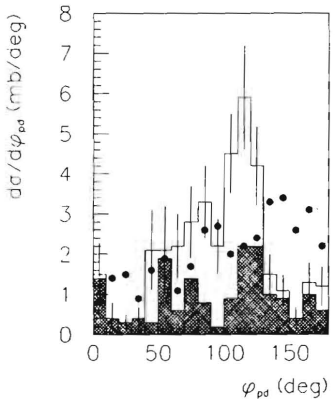

Fig 4a

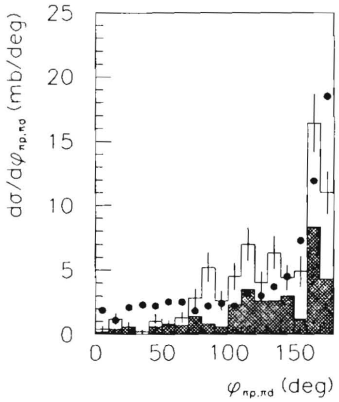

Fig 4b

Fig. 4. Azimuthal angle φ_{ij} distributions of the secondary particles in C.M.S (a) and L.S. (b). The points as in fig 1.